Journal of The Electrochemical Society, **158** (1) D1-D5 (2011)
0013-4651/2010/158(1)/D1/5/$28.00 © The Electrochemical Society

Atomic Layer Deposition of Ni Thin Films and Application to Area-Selective Deposition

Woo-Hee Kim,[a] Han-Bo-Ram Lee,[b] Kwang Heo,[c] Young Kuk Lee,[e] Taek-Mo Chung,[e] Chang Gyoun Kim,[e] Seunghun Hong,[c,d] Jong Heo,[a] and Hyungjun Kim[b,*,z]

[a]*Department of Material Science and Engineering, Pohang University of Science and Technology, Pohang 790-784, Korea*
[b]*School of Electrical and Electronic Engineering, Yonsei University, Seoul 120-749, Korea*
[c]*Department of Physics and Astronomy and* [d]*Interdisciplinary Program in Nano-Science and Technology, Seoul National University, Seoul 151-747, Korea*
[e]*Advanced Materials Division, Korea Research Institute of Chemical Technology, Daejeon 305-600, Korea*

Ni thin films were deposited by atomic layer deposition (ALD) using bis(dimethylamino-2-methyl-2-butoxo)nickel [$Ni(dmamb)_2$] as a precursor and NH_3 gas as a reactant. The growth characteristics and film properties of ALD Ni were investigated. Low-resistivity films were deposited on Si and SiO_2 substrates, producing high-purity Ni films with a small amount of oxygen and negligible amounts of nitrogen and carbon. Additionally, ALD Ni showed excellent conformality in nanoscale via holes. Utilizing this conformality, Ni/Si core/shell nanowires with uniform diameters were fabricated. By combining ALD Ni with octadecyltrichlorosilane (OTS) self-assembled monolayer as a blocking layer, area-selective ALD was conducted for selective deposition of Ni films. When performed on the prepatterned OTS substrate, the Ni films were selectively coated only on OTS-free regions, building up Ni line patterns with 3 μm width. Electrical measurement results showed that all of the Ni lines were electrically isolated, also indicating the selective Ni deposition.
 [DOI: 10.1149/1.3504196]

Manuscript submitted December 15, 2009; revised manuscript received July 16, 2010. Published November 9, 2010.

As scaling continues in order to improve device integration in the complementary metal-oxide-semiconductor (CMOS) process, the silicidation process becomes more essential for lowering contact resistance and increasing drive currents.[1] $TiSi_2$ and $CoSi_2$ have been extensively investigated as contact materials. However, these materials have been reported to cause increased series resistance of devices at the sub-65 nm technology node.[2] In addition, $TiSi_2$ exhibits the narrow line effect.[3] Although $CoSi_2$ lines depend less on the sheet resistance, the greater consumption of Si is a major concern in forming silicide with the decreased junction depth. Also, both materials require a two-step annealing process to form a low resistive phase.[3] Because of these problems, NiSi is being investigated as a contact material for application in nanoscale devices and shows no linewidth effects, low resistivity, low Si consumption, low process temperature, and a one-step annealing process.[4]

The Ni metal deposition process is a key requirement in the formation of Ni silicide contacts. Among the various thin film deposition techniques, atomic layer deposition (ALD) is a promising method which exhibits good conformality and uniformity, atomic scale thickness controllability, and low impurity contamination at a low growth temperature due to its growth mechanism based on a self-limited surface reaction.[5-7] However, in spite of its importance in nanoscale device contact applications, there are only a few reports on the ALD of Ni films.[2,8-13] In an early study, Chae et al. reported the formation of Ni films by H_2 plasma reduction of ALD NiO films using bis(cyclopentadienyl)nickel [$NiCp_2$] as a precursor and water as a reactant.[9] Later, Do et al. reported a Ni ALD process using a $Ni(dmamb)_2$ precursor and H_2 as the reactant gas.[2] However, the Ni films deposited in these studies contain a large amount of carbon, which may have caused high resistivity.[2,9] These results suggest that a combination of a proper precursor and reactant should be introduced to produce pure metal Ni films with low resistivities.

In addition, area-selective ALD (AS-ALD) using self-assembled monolayers (SAMs) is attracting attention because it is simple and requires no expensive patterning processes, such as lithography and etching. Several groups have utilized AS-ALD for various applications, such as fuel cell and solar cell fabrication.[14,15] The surface properties of the films can be hydrophobic or hydrophilic, depending on the end groups of the SAMs. Previous studies on AS-ALD have been limited to research fields of some oxide materials, such as ZrO_2, HfO_2, ZnO, and TiO_2.[16-21] AS-ALD processes for metal have only been reported for Ru, Pt, and Ir, all of which are deposited using O_2 gas as a reactant.[22-25] AS-ALD using other reactant gases such as NH_3 or H_2 has rarely been studied.[26] Recently, we have reported the AS-ALD of Co using bis(N,N'-diisopropylacetamidinato)cobalt(II) [$Co(iPr\text{-}AMD)_2$] as a precursor and NH_3 and H_2 as reactants.[27]

For this study, we developed a new Ni ALD process utilizing $Ni(dmamb)_2$ as a Ni precursor and NH_3 gas as a reactant. The ALD Ni films showed low resistivity and contained only a minimal amount of oxygen and no nitrogen and carbon.[2,9] Notably, nitrogen and other impurities were not incorporated into the Ni films in spite of using the NH_3 reactant. Additionally, the ALD Ni process was applied to AS-ALD using octadecyltrichlorosilane (OTS) SAM as a blocking layer. The ALD Ni films were selectively deposited onto the prepatterned OTS lines, forming well-defined Ni lines.

Experimental

For this study, a commercial ALD chamber (Quros Plus 150) with a loadlock chamber was used. This system had a double shower head system for better uniformity. Further information on the chamber configuration can be found in our previous report.[28] The Ni precursor $Ni(dmamb)_2$ was contained in a stainless steel bubbler maintained at a temperature of 70°C to produce a suitable vapor pressure. The $Ni(dmamb)_2$ molecules generated were carried into the main chamber by Ar carrier gas at a flow rate of 50 sccm. Ar gas at the same flow rate was also used for purging the excess gas molecules and by-products between each precursor and exposure step. For ALD Ni, the NH_3 gas reactant at a flow rate of 400 sccm was delivered to the reaction chamber. The substrate temperature was maintained at 300°C. One ALD deposition cycle consisted of four steps: $Ni(dmamb)_2$ precursor exposure (t_s), Ar purging (t_p), NH_3 gas reactant exposure (t_r), and another Ar purging (t_p). The times t_s and t_p were fixed at 4 and 1 s, respectively, and t_r was systematically varied from 2 to 12 s. Si(001) and SiO_2(100 nm)/Si(001) substrates were used. The Si(001) substrates were cleaned by dipping in a buffered oxide etchant (6:1) for 10 s, followed by a deionized (DI) water rinsing and N_2 blowing, resulting in

* Electrochemical Society Active Member.
z E-mail: hyungjun@yonsei.ac.kr

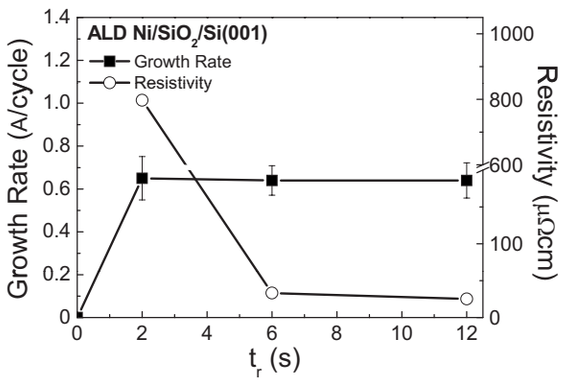

Figure 1. Dependence of the film growth rate and resistivity on the exposure time of NH_3 gas (t_r) to SiO_2 substrate.

H-terminated Si. The SiO_2 substrates were cleaned in acetone, isopropyl alcohol, and DI water, followed by N_2 blowing, resulting in OH-terminated SiO_2.

For AS-ALD, OTS-coated substrates were prepared. The SiO_2(200 nm)/Si(001) substrate was cleaned with a piranha solution (H_2SO_4/H_2O_2 = 4:1, by volume ratio), resulting in a Si substrate coated with 2–3 nm of chemical oxide. Subsequently, the substrate was dipped in diluted OTS solution (toluene/OTS = 10 mL:25 μl) for 24 h in a glove box for OTS coating. To prepattern the OTS coating with lines, a photography-assisted process was employed as follows. The SiO_2/Si substrate was cleaned with the same piranha solution. Photoresist (PR) (AZ5214) patterning was conducted by photolithography, followed by dipping in the OTS solution for 10 minutes at room temperature with a humidity of about 80% for selective OTS coating on the PR-free region. Then, the remaining PR was removed by acetone. An additional description of the preparation of patterned OTS substrates can be found in Fig. 1 of our earlier report.[27] After preparation of the OTS-coated substrates, the ALD Ni process was performed at 300°C (T_s) for t_r = 6 s.

Field emission scanning electron microscopy (FE-SEM) was used to determine the film thickness, morphology, and conformality. The resistivities of the ALD Ni thin films were calculated using the film thickness and sheet resistance measured by four-point probe. The microstructures of the Ni films were analyzed by synchrotron radiation x-ray diffraction (SRXRD, Pohang Acceleration Laboratory, 3C2 beam line). The chemical compositions were analyzed by x-ray photoelectron spectroscopy (XPS). The deposition selectivity of ALD Ni on line-patterned OTS substrates was estimated by measuring the thickness difference between the OTS-coated and uncoated regions using atomic force microscopy (AFM) and profilometry (α-step). In addition, the *I–V* characteristics of AS-ALD Ni on the prepatterned OTS surface were measured using an HP 5270A.

Results and Discussion

The growth characteristics and film properties of ALD Ni.— Figure 1 shows the dependence of the growth rate of the ALD Ni films on SiO_2(100 nm)/Si for each cycle and the resistivity value at NH_3 gas exposure times (t_r) from 2 to 12 s at T_s = 300°C. The growth rates were saturated at $t_r > 2$ s, indicating that the films grew through self-limited surface reactions, which is a typical ALD characteristic.[5] The saturated growth rate was 0.64 Å/cycle, and the lowest resistivity was about 25 μΩ cm at t_r = 12 s, which is the lowest value of resistivity ever reported for ALD Ni.[2,9] In addition, 50 nm thick Ni films (800 cycles) were well deposited on the H-terminated Si substrate and OH-terminated SiO_2/Si substrate, as

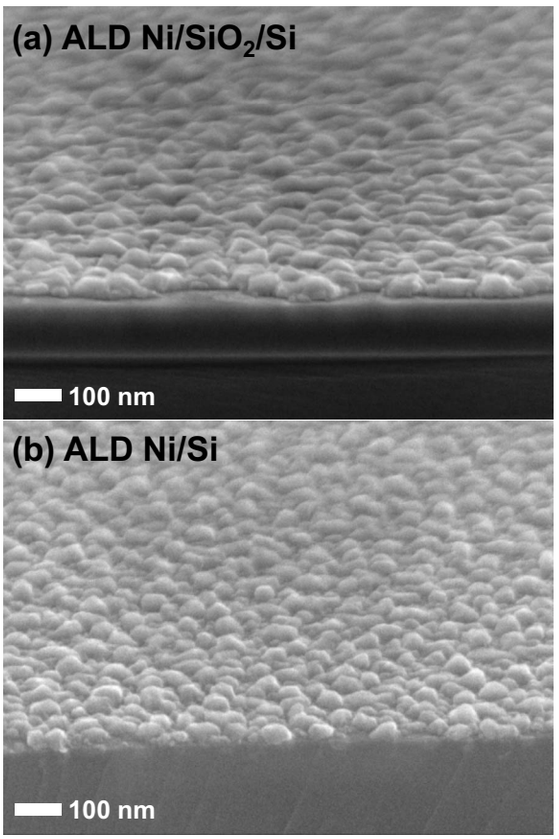

Figure 2. FE-SEM images of ALD Ni films on (a) SiO_2 substrate and (b) Si substrate.

shown in the FE-SEM images in Figs. 2a and b, indicating the absence of substrate dependency toward surface functional groups, such as hydroxyls.

To analyze the chemical composition, the ALD Ni film on SiO_2 of Fig. 2a was analyzed by XPS. Ni core level XPS peaks were primarily observed at 852.7 and 870 eV of binding energy, consistent with the $2p_{3/2}$ and $2p_{1/2}$ peaks of metallic Ni in Fig. 3a.[29] In addition, the broad peak observed at 858.7 eV is the main 6 eV satellite peak, which is due to a two hole $c3d^9 4s^2$ (c is a core hole) final state effect.[30] From the XPS spectra related to impurities, shown in Fig. 3b, negligible amounts of nitrogen and carbon were detected. Meanwhile, a relatively weak and broad peak related to some bonded oxygen was observed for O 1s. To elucidate this peak, the O 1s peak was deconvoluted to two peaks, each of which corresponds to NiO at 530 eV and $Ni(OH)_2$ at 531.5 eV.[29,31] The molecular structure of the $Ni(dmamb)_2$ is composed of Ni atom directly bonded to two neighboring N and O atoms. Thus, a small amount of oxygen incorporation in the ALD Ni film is probably due to the incomplete elimination of directly bonded O atoms. Although the film contained a tiny amount of impurities, to our knowledge, this is the first report on ALD Ni producing pure Ni metal films with low resistivity. Although two research groups published results on the ALD Ni process, the Ni films contained significant amounts of carbon and low levels of oxygen due to the absence of adequate reactant, which would effectively eliminate the ligands from the Ni precursor.[2,9]

Figures 4a and b show the XRD patterns of 30 nm thick Ni films grown on $Ni(dmamb)_2$ and Si substrates, respectively. The XRD results indicate that both samples were polycrystalline metallic Ni thin films with a face-centered cubic microstructure but had different preferred crystal orientations: (111) on the Si substrate and (002) on

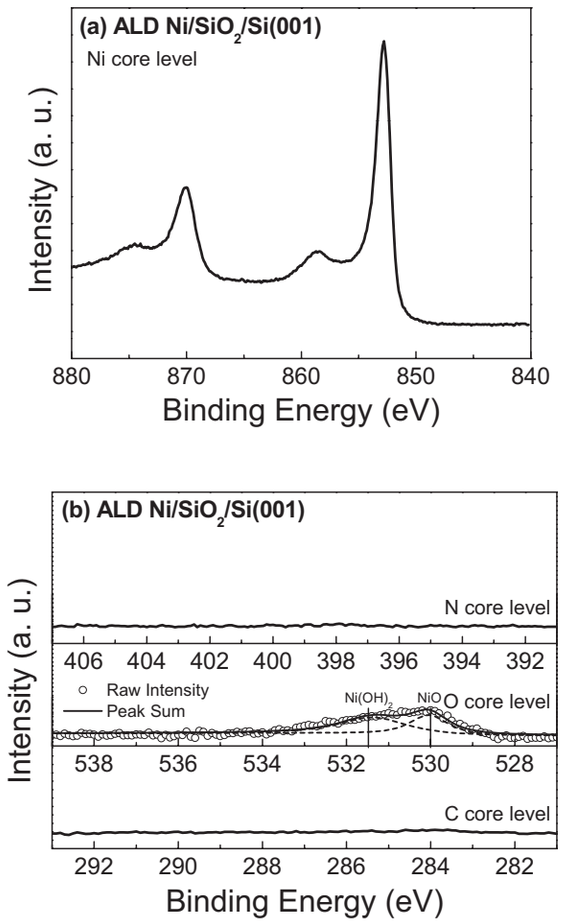

Figure 3. XPS spectra of ALD Ni film: (a) Ni core level and (b) impurity content (N, O, and C) core levels.

the SiO_2 substrate. No second phase related to carbon and oxygen was observed. Generally, significant amounts of carbon impurities in a film may cause high resistivity. In that case, if the incorporated carbon forms the Ni_3C phase, lower resistivity can be achieved than with a randomly distributed carbon.[2] However, our ALD Ni process excludes this possibility since the XPS results show a minimal amount of carbon contamination.

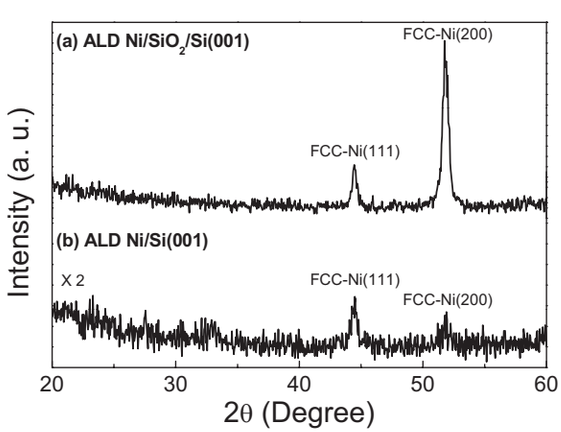

Figure 4. SRXRD patterns of 30 nm thick Ni films grown on (a) SiO_2 and (b) Si (SRXRD, Pohang Acceleration Laboratory, 3C2 beam line).

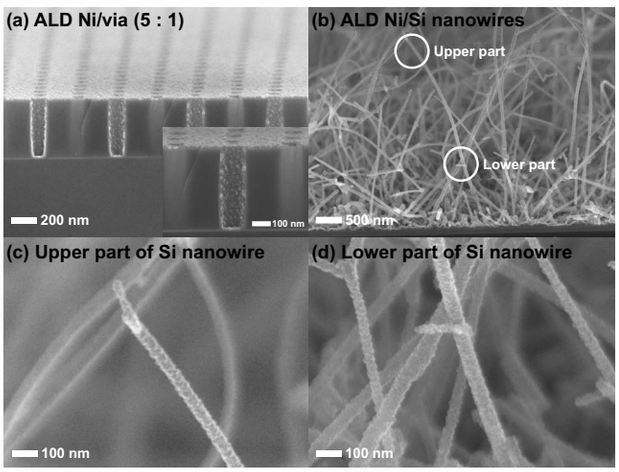

Figure 5. FE-SEM images of the ALD Ni films on (a) a nanosize via hole pattern with an aspect ratio of 5:1 (inset: magnified image), (b) Si nanowire, (c) upper, and (d) lower part of the Si nanowire.

To confirm the good conformality of the current ALD Ni process, we deposited Ni inside via holes and on top of chemical vapor deposition grown Si nanowires. Figure 5a shows the cross-sectional FE-SEM images of 20 nm thick Ni films grown in nanoscale contact hole vias with an aspect ratio of 5:1 (depth of 450 nm and diameter of 90 nm). Excellent conformality of the ALD Ni films was observed in the via holes. The Ni film thicknesses on the top, side wall, and bottom of the via were all ~20 nm (Fig 5a). Figure 5b shows ALD Ni film covered Si nanowires with diameters of 20 nm. The upper part of the Ni film on the nanowires had the same thickness as the lower part of the Si nanowires, as shown in Figs. 5c and d. These results indicate that we produced Ni/Si core/shell nanowires with uniform thickness of the outer Ni shell. This cannot be achieved using other deposition techniques, such as physical vapor deposition.

Area-selective ALD Ni using OTS SAM.— We applied a current Ni ALD process to AS-ALD using OTS SAM. First, we prepared two kinds of substrates: OTS-coated and uncoated substrates (as stated in the Experimental section). The Ni ALD was carried out on both substrates, and the corresponding SEM images are shown in Fig. 6. The Ni film was deposited onto the uncoated substrate (Fig. 6a) in contrast to the OTS-coated substrate (Fig. 6b), indicating that the OTS effectively blocked Ni film deposition.

Additionally, the AS-ALD of Ni was conducted on a substrate with prepatterned OTS. Line patterns were formed by conventional photolithography, consisting of an alternately exposed OTS-coated region of 9 μm width and an uncoated region of 3 μm width. Figure 7a is an AFM image showing the ALD Ni film deposited on the prepatterned OTS-coated substrate. The width of the deposited Ni lines and the distance between them are 3 and 9 μm, respectively, replicating the OTS patterns inversely. The thickness profile of AS-ALD Ni in Fig. 7b also indicates that the films were selectively deposited on the uncoated region. In addition, the width of the Ni lines and the distance between them were similar to those in the AFM image in Fig. 7a.

The film quality of AS-ALD Ni was evaluated by current–voltage (*I–V*) measurements using two-point probes (HP 5270A). First, two electrical probes were placed on the same line 100 μm apart. A linear increase in current was observed with increased applied voltage, indicating that an ohmic electrical contact was established (longer line in Fig. 8). When the distance between the electrical probes was reduced to 50 μm, ohmic electrical contact was also shown (shorter line in Fig. 8). In this case, the slope of the *I–V* curve for the Ni line was approximately doubled compared to that

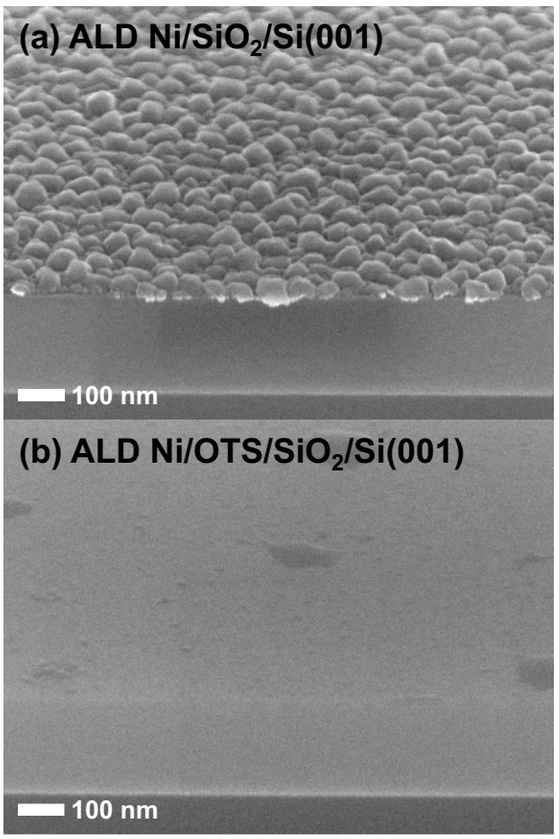

Figure 6. The FE-SEM images of ALD Ni films on (a) OTS-uncoated and (b) OTS-coated substrates.

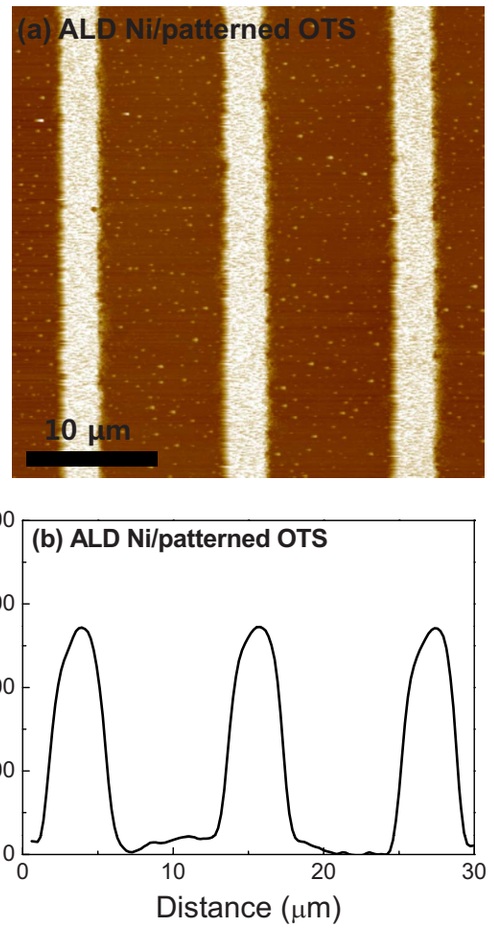

Figure 7. (Color online) AS-ALD Ni films deposited on prepatterned OTS-coated substrate: (a) AFM image and (b) thickness profile.

for the 100 μm distance. In both cases, the resistivity of the Ni line was calculated to be about 96 μΩ cm using the simple equation AR = ρL, assuming that the cross-section of the Ni line was rectangular in shape, where A is the cross-sectional area of the line, which is obtained by multiplying the film thickness (32 nm) with the line width (3 μm), R is the resistance of the Ni line calculated from the linear *I–V* curve, and L is the line length between the two probes (longer line: 100 μm; shorter line: 50 μm). The resistivity of the Ni line calculated using this equation was higher than that of the ALD Ni film measured by four-point probe. The increase in resistivity compared to that in the Ni thin film cannot be due to surface scattering effects, because the dimensions of the Ni lines were much larger than the electron scattering length in Ni (about 10 Å).[32] Also, since a similar resistivity was obtained regardless of the line length between the probes, we excluded the effects of parasitic resistances, such as the contact resistance and the spreading resistance caused by the two-point probe method. Thus, we attributed the increased resistivity to the incorporation of impurities during the deposition of the films on the PR-patterned substrate. Also, a negligible current was detected on different Ni lines, implying that the Ni lines were electrically isolated from each other. Therefore, we can assert that the Ni film was not formed on OTS-coated regions.

Conclusions

In this study, we investigated an ALD Ni process using a $Ni(dmamb)_2$ precursor and NH_3 gas and applied it to AS-ALD onto a substrate with lines patterned with OTS SAM as a blocking layer. ALD Ni exhibited good self-saturation growth characteristics without substrate dependency on Si or SiO_2 and produced pure and low-resistive Ni films mainly due to the efficient removal of $Ni(dmamb)_2$ ligands using NH_3 gas. In addition, ALD Ni showed excellent conformality on nanoscale 3D structures, such as via holes and Si nanowires. For selective deposition, by combining ALD Ni and OTS SAM, Ni AS-ALD was successfully established without an etching process on the line-patterned OTS substrate. Regularly patterned Ni line films showed ohmic electrical contact properties, sug-

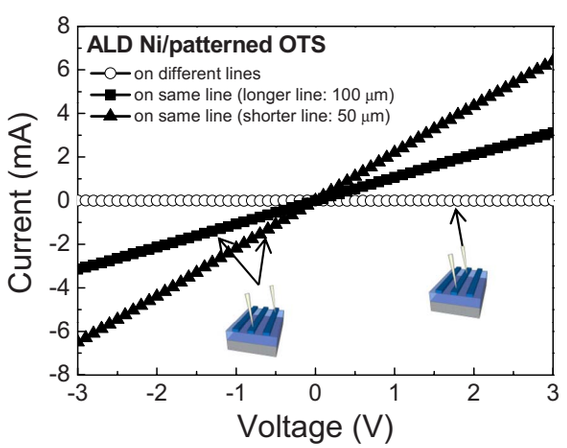

Figure 8. (Color online) *I–V* measurements of AS-ALD Ni on different lines (○), same line with 100 μm distance (■), and 50 μm distance (●). (Inset: drawings showing probes on Ni lines.)

gesting applicability of our process to the current CMOS device process as a simple and cheap alternative to the lithography-based patterning process.

Acknowledgments

This work was supported by the Technology Innovation Program (Industrial Strategic Technology Development Program, 10035430, Development of reliable fine-pitch metallization technologies) funded by the Ministry of Knowledge Economy (MKE, Korea). The FE-SEM and the synchrotron XRD analyses were performed at the National Center for Nanomaterials and Technology (NCNT) and the 3C2 x-ray scattering beam line at the Pohang Acceleration Laboratory (PAL), respectively.

Yonsei University assisted in meeting the publication costs of this article.

References

1. D. X. Xu, S. R. Das, C. J. Peters, and L. E. Erickson, *Thin Solid Films*, **326**, 143 (1998).
2. K. Do, C. Yang, I. Kang, K. Kim, K. Back, H. Cho, H. Lee, S. Kong, S. Hahm, and D. Kwon, *Jpn. J. Appl. Phys., Part 1*, **45**, 2975 (2006).
3. Y. Hu and S. P. Tay, in *The First International Conference on Advanced Materials and Processes for Microelectronics*, p. 2284 (1999).
4. J. A. Kittl, A. Lauwers, O. Chamirian, M. Van Dal, A. Akheyar, M. De Potter, R. Lindsay, and K. Maex, *Microelectron. Eng.*, **70**, 158 (2003).
5. H. Kim, *J. Vac. Sci. Technol. B*, **21**, 2231 (2003).
6. H. Kim, *Surf. Coat. Technol.*, **200**, 3104 (2006).
7. T. Aaltonen, P. Alen, M. Ritala, and M. Leskelae, *Chem. Vap. Deposition*, **9**, 45 (2003).
8. B. S. Lim, A. Rahtu, and R. G. Gordon, *Nature Mater.*, **2**, 749 (2003).
9. J. Chae, H. S. Park, and S. Kang, *Electrochem. Solid-State Lett.*, **5**, C64 (2002).
10. M. Daub, M. Knez, U. Goesele, and K. Nielsch, in *10th Joint MMM/INTERMAG Conference*, p. 09J111 (2007).
11. Y. Chung-Mo, Y. Sang-Won, H. Jong-Bong, N. Kyung-Il, C. Hyun-Ick, L. Heon-Bok, J. Jeong, K. Sung-Ho, H. Sung-Ho, and J. Lee, *Jpn. J. Appl. Phys., Part 1*, **46**, 1981 (2007).
12. M. Utriainen, M. Kröger-Laukkanen, L.-S. Johansson, and L. Niinistö, *Appl. Surf. Sci.*, **157**, 151 (2000).
13. J. Ha, S. Yun, and J. Lee, *Curr. Appl. Phys.*, **10**, 41 (2010).
14. X. Jiang, H. Huang, F. B. Prinz, and S. F. Bent, *Chem. Mater.*, **20**, 3897 (2008).
15. C. Bae, H. Yoo, S. Kim, K. Lee, J. Kim, M. M. Sung, and H. Shin, *Chem. Mater.*, **20**, 756 (2008).
16. R. Chen, H. Kim, P. C. McIntyre, D. W. Porter, and S. F. Bent, *Appl. Phys. Lett.*, **86**, 191910 (2005).
17. R. Chen, H. Kim, P. C. McIntyre, and S. F. Bent, *Appl. Phys. Lett.*, **84**, 4017 (2004).
18. J. P. Lee and M. M. Sung, *J. Am. Chem. Soc.*, **126**, 28 (2004).
19. R. Chen, H. Kim, P. C. McIntyre, and S. F. Bent, *Chem. Mater.*, **17**, 536 (2005).
20. B. H. Lee and M. M. Sung, *J. Nanosci. Nanotechnol.*, **7**, 3758 (2007).
21. E. K. Seo, J. W. Lee, H. M. Sung-Suh, and M. M. Sung, *Chem. Mater.*, **16**, 1878 (2004).
22. K. J. Park, J. M. Doub, T. Gougousi, and G. N. Parsons, *Appl. Phys. Lett.*, **86**, 051903 (2005).
23. R. Chen and S. F. Bent, *Adv. Mater.*, **18**, 1086 (2006).
24. R. Chen and S. F. Bent, *Chem. Mater.*, **18**, 3733 (2006).
25. E. Farm, M. Kernell, M. Ritala, and M. Leskel, *Chem. Vap. Deposition*, **12**, 415 (2006).
26. A. Dube, M. Sharma, P. F. Ma, and J. R. Engstrom, *Appl. Phys. Lett.*, **89**, 164108 (2006).
27. H.-B.-R. Lee, W.-H. Kim, J. W. Lee, J.-M. Kim, K. Heo, I. C. Hwang, Y. Park, S. Hong, and H. Kim, *J. Electrochem. Soc.*, **157**, D10 (2010).
28. W.-H. Kim, S.-J. Park, J.-Y. Son, and H. Kim, *Nanotechnology*, **19**, 045302 (2008).
29. J. F. Moulder, W. F. Stickle, P. E. Sobol, and K. D. Bomben, *Handbook of X-ray Photoelectron Spectroscopy*, Perkin-Elmer Corporation, Minnesota (1992).
30. A. P. Grosvenor, M. C. Biesinger, R. S. C. Smart, and N. S. McIntyre, *Surf. Sci.*, **600**, 1771 (2006).
31. T. L. Barr, *J. Phys. Chem.*, **82**, 1801 (1978).
32. D. T. Pierce and H. C. Siegmann, *Phys. Rev. B*, **9**, 4035 (1974).